

Controlling Vibrational Excitations in C_{60} by Laser Pulse Durations

G. P. Zhang¹ and Thomas F. George²

¹*Department of Physics, Indiana State University, Terre Haute, Indiana 47809, USA*

²*Office of the Chancellor/Departments of Chemistry & Biochemistry and Physics & Astronomy,
University of Missouri-St. Louis, St. Louis, Missouri 63121, USA*

(Received 11 April 2004; published 27 September 2004)

Two similar off-resonant ultrafast laser experiments in C_{60} have reported two different vibrational modes that dominate the relaxation process: one predicts the A_g modes while the other the H_g modes. A systematical simulation presented here reveals that this experimental discrepancy results from the laser pulse duration. The numerical results show that since each mode ν has a distinctive optimal duration τ_ν^o , the A_g modes are strongly suppressed for durations longer than 40 fs, while the H_g modes start to grow. For the off-resonant and low-intensity excitations, the period Ω_ν^o of the dominant mode and τ_ν^o satisfy the relation $\Omega_\nu^o/\tau_\nu^o \approx 3.4$. By carefully scanning the laser frequencies and pulse durations, a comprehensive excitation diagram is constructed, which can be used to guide experiments to selectively excite the A_g and H_g modes in C_{60} by an ultrafast laser. Its potential impact is also discussed.

DOI: 10.1103/PhysRevLett.93.147401

PACS numbers: 78.66.Tr, 42.65.Re

Ultrafast lasers present an unprecedented opportunity to investigate electron and phonon dynamics in the time domain. Since the lattice interacts with light through electrons, the electron-phonon interaction can be probed directly. This provides valuable information about dynamics in semiconductors [1], superconductors [2,3], C_{60} [4–7], and other nanostructures, but the practical challenges are enormous. Experimentally, the laser frequency, intensity, and pulse duration all influence the dynamics. For instance, an early experiment in C_{60} by Dexheimer *et al.* [4] showed that two A_g modes dominate the transmittance change. By contrast, Bhardwaj *et al.* [5], Hohmann *et al.* [6] and, very recently, Boyle *et al.* [7] suggested it is the H_g modes, not A_g modes, that dominate the relaxation process. It is unclear at the present as to what leads to this discrepancy. However, C_{60} is not alone. For superconductors, only a very few experiments [3] are able to detect the phonon coherence though the experimental conditions are similar. These inconsistencies substantially hamper ongoing investigations on superconductors and nanostructures. A clear understanding of vibrational excitations is “a must”.

Motivated by the above experimental results, in this Letter we perform a dynamical simulation in C_{60} to resolve the experimental discrepancy and examine how one can selectively control a few A_g and H_g mode excitations. Our results show that although the experimental results do not agree among themselves, the discrepancy precisely suggests a novel scheme to control phonon excitations. In particular, when excited at off resonance, for a laser duration shorter than 20 fs, the $A_g(1)$ and $A_g(2)$ modes dominate, but for a duration longer than 40 fs, the H_g modes dominate. For the off-resonant and weak intensity excitations, the dominant mode’s period Ω^o and optimal laser duration τ_o , fulfill the relation $\Omega^o/\tau_o \approx 3.4$. Scanning through both frequencies and pulse durations, we construct a systematic mode-excitation dia-

gram, which will facilitate the experimental efforts to target a few phonon modes. This may pave the way to explore processes like Cooper pair breaking.

C_{60} is simulated by the Hamiltonian [8]

$$H_0 = -\sum_{ij,\sigma} t_{ij}(c_{i,\sigma}^\dagger c_{j,\sigma} + \text{H.c.}) + \frac{K_1}{2} \sum_{i,j} (r_{ij} - d_0)^2 + \frac{K_2}{2} \sum_i d\theta_{i,5}^2 + \frac{K_3}{2} \sum_i (d\theta_{i,6,1}^2 + d\theta_{i,6,2}^2), \quad (1)$$

where $c_{i,\sigma}^\dagger$ is the electron creation operator at site i with spin σ ($=\uparrow\downarrow$) [9]. The first term on the right hand side represents the electron hopping, where $t_{ij} = t^0 - \alpha(|\mathbf{r}_i - \mathbf{r}_j| - d_0)$ is the hopping integral between nearest-neighbor atoms at \mathbf{r}_i and \mathbf{r}_j , and $r_{ij} = |\mathbf{r}_i - \mathbf{r}_j|$. Here t^0 is the average hopping constant, and α is the electron-lattice coupling constant. The last three terms on the right hand side are the lattice stretching, pentagon-hexagon, and hexagon-hexagon bending energies, respectively. By fitting the energy gap, bond lengths, and normal mode frequencies, You *et al.* [8] have determined the above parameters as $t^0 = 1.91$ eV, $\alpha = 5.0$ eV/Å, $K_1 = 42$ eV/Å², $K_2 = 8$ eV/rad², $K_3 = 7$ eV/rad², and $d = 1.5532$ Å. These parameters will be fixed in our calculation [10].

The dynamical process is simulated by including the laser field, which is described by $H_I = -e\sum_{i\sigma} \mathbf{E}(t) \cdot \mathbf{r}_i n_{i\sigma}$, where $n_{i\sigma}$ is the electron number operator and $|\mathbf{E}(t)| = A \cos[\omega(t - t_0)] \exp[-(t - t_0)^2/\tau^2]$ [11]. Here A , ω , τ , e , t , and t_0 are the field amplitude, laser-frequency, pulse duration or width, electron charge, time, and time delay, respectively. We numerically solve the Liouville equation for the electron density matrices [11,12], $-i\hbar\partial\langle\rho_{ij}^\sigma\rangle/\partial t = \langle[\rho_{ij}^\sigma, H]\rangle$, where $H = H_0 + H_I$, $\rho_{ij}^\sigma = c_{i\sigma}^\dagger c_{j\sigma}$ is the density matrix operator, and $\langle\rangle$ represents the expectation value. We treat the carbon atoms classically as before [12,13], and neither the bending nor

the lattice stretching terms enter the Liouville equation. After solving the Liouville equation, we are ready to investigate vibrational excitations.

To determine how strongly the normal modes are excited, we need to find a way to quantitatively characterize them. Upon first glance, the potential energy appears a natural choice, but upon laser excitation, the potential surface $V(\{\mathbf{r}\})$ becomes so anharmonic that the harmonic expansion is not sufficient, and higher-order terms become significant $V(\{\mathbf{r}\}) = V(\{\mathbf{r}_0\}) + \frac{1}{2!} \sum_{ij} \frac{\partial^2 V}{\partial r_i \partial r_j} \Delta r_i \Delta r_j +$ higher-order terms. In order to solve this problem, instead of expanding the potential energy in terms of normal modes, we expand the kinetic energy. Since the kinetic energy is always a quadratic function of velocity and has no such higher-order terms, independent of laser intensity, the kinetic energy K can always be exactly expanded as $K = \sum_{\nu} K_{\nu} = \sum_{\nu} \frac{m}{2} dQ_{\nu}^2$, where K_{ν} is the kinetic energy for mode ν , and m is the mass of carbon atom. $dQ_{\nu} = \sum_i \mathbf{V}(i) \cdot \mathbf{G}_{\nu}(i)$, where $\mathbf{V}(i)$ and $\mathbf{G}_{\nu}(i)$ are the velocities of atom i and the normal mode eigenvector of mode ν , respectively. Our experience shows that this method works extremely well in practice [14].

Before we present our numerical results, let us first look at the experimental findings. Dexheimer *et al.* [4] used a laser pulse with duration of 12 fs and wavelength of 620 nm to excite C_{60} and found only two A_g modes visible in their transmittance change. In our simulation, we use the same laser frequency and pulse width. We choose the laser field amplitude $A = 0.05 \text{ eV/\AA}$ [15]. In Fig. 1(a) we show the respective kinetic energies $K_{A_g(1)}$ and $K_{A_g(2)}$ for the $A_g(1)$ and $A_g(2)$ modes as a function of time. Upon laser excitation, both modes oscillate at their distinctive periods [67 fs for $A_g(1)$ and 23 fs for $A_g(2)$] [16], which is fully consistent with the experimental results. $A_g(2)$ responds much more quickly because of its higher frequency, and exhibits some beating around 0 fs. It gains its maximal kinetic energy around 10 fs, then decays slightly, and after 20 fs it oscillates periodically with a constant amplitude. The $A_g(1)$ mode behaves similarly, except that it reaches its maximum after 35 fs.

We are interested in understanding why the H_g modes do not show up in the experiment. Figure 1(b) shows the results for the two strongest H_g modes [$H_g(5)$]. Note that those dominant H_g modes gain less than $0.5 \times 10^{-6} \text{ eV}$, which is 5 times smaller than $K_{A_g(1)}$. Although this result is already consistent with the experiment, to be more convincing, we have examined all relevant parameters. Since in our simulation almost all the parameters are determined by either the experiment or the previous theory, the only adjustable parameter is the laser intensity [15]. Is it possible that the laser intensity could enhance H_g modes so that K_{H_g} is larger than K_{A_g} ? When we increase the laser intensity, we find a dramatic change in the kinetic energies among those normal modes. In the

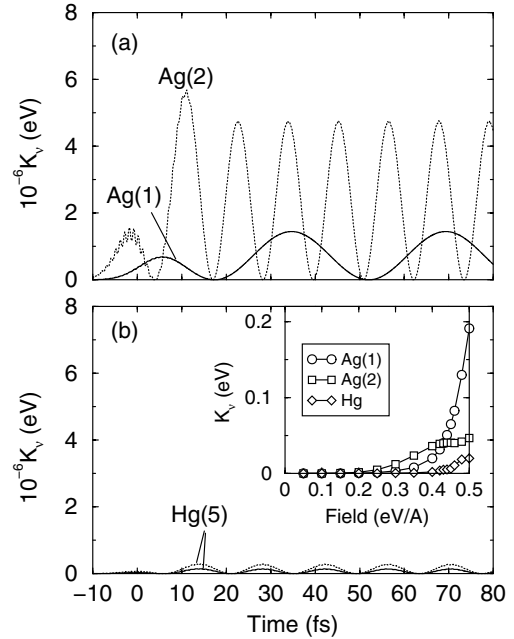


FIG. 1. (a) Kinetic energies K_{ν} for the modes $A_g(1)$ and $A_g(2)$ as a function of time. The laser frequency is $\omega = 2.0 \text{ eV}$ and intensity is 0.05 eV/\AA . (b) Kinetic energies for the H_g modes. These modes gain a very small kinetic energy. Inset: Dependence of K_{ν} on the laser intensity for three different modes.

inset of Fig. 1(b), for each mode we plot the kinetic energy versus the field intensity. For a small laser intensity, $K_{A_g(2)}$ is always larger than $K_{A_g(1)}$. Since $K_{A_g(1)}$ increases exponentially with intensity and $K_{A_g(2)}$ starts to saturate after 0.4 eV/\AA , there is a crossover between $K_{A_g(1)}$ and $K_{A_g(2)}$ at about 0.42 eV/\AA [17]. On the other hand, although K_{H_g} increases with intensity, the H_g modes still can not compete with the $A_g(1)$ mode (see inset of Fig. 1) [18]. This explains the absence of H_g modes in the experiment.

However, the above experimental result contradicts the experimental finding by Bhardwaj *et al.* [5], Hohmann *et al.* [6], and Boyle *et al.* [7] who showed the H_g , not A_g , modes dominate. This is very puzzling. Although Dexheimer and Bhardwaj both excited the system at off resonance, their wavelengths are not exactly the same. Would it be possible that this small wavelength difference accounts for the discrepancy? By scanning the frequencies from 0.5 (including Bhardwaj's frequency of 0.69 eV) to 2.0 eV (Dexheimer's frequency) with a laser intensity of 0.05 eV/\AA and pulse duration of 12 fs, we could not find a case dominated by the H_g mode. These results suggest that the laser frequency and intensity are unlikely to be the main source of the experimental discrepancy. Extensive studies by other research groups [19] finally help us to single out the only possible reason: the laser pulse duration.

It is indeed true that different pulse durations were used in all four experiments: Dexheimer *et al.* used a duration of 12 fs [4], while Boyle *et al.* [5], Hohmann *et al.* [6], and Bhardwaj *et al.* [7] used 100 fs, 90 fs, and 70 fs, respectively. We use Bhardwaj's wavelength at 1800 nm or 0.69 eV. (The results for $\omega = 2$ eV are similar.) The laser intensity is 0.05 eV/Å. We systematically change the pulse duration from 5 fs to 100 fs. The maximal kinetic energies K_ν^{\max} [20] are shown in Fig. 2(a), where $K_{A_g(1)}$ and $K_{A_g(2)}$ are denoted by empty circles and boxes, respectively. Except for those first two solid circles, which denote the $H_g(8)$ and $H_g(5)$ modes, the other solid circles represent the $H_g(1)$ mode only. Figure 2(a) reveals a truly insightful picture. (1) With the shortest duration τ (~ 5 fs), only high-frequency modes are strongly excited. In our present case, they are $A_g(2)$, $H_g(8)$, and $H_g(5)$. (2) A longer duration weakens high-frequency modes but enhances low-frequency modes. In particular, the $A_g(1)$ mode starts to grow and peaks at 22.5 fs. For $15 \text{ fs} < \tau < 40 \text{ fs}$, $A_g(1)$ dominates. (3) For $100 \text{ fs} > \tau > 40 \text{ fs}$, $H_g(1)$ dominates over all other modes.

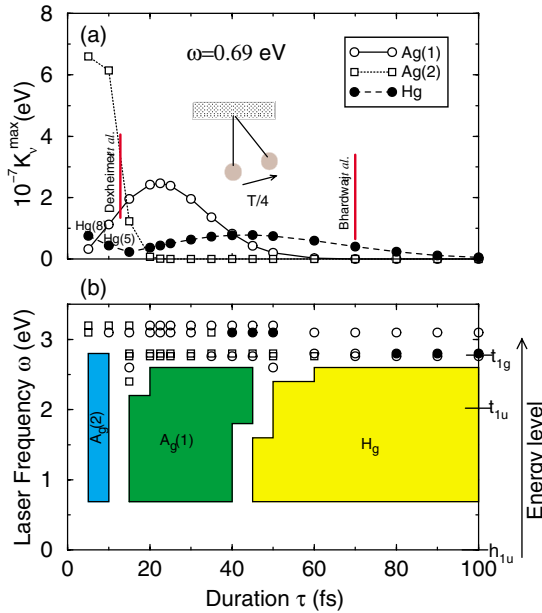


FIG. 2 (color online). (a) Dependence of the maximal kinetic energy K_ν^{\max} on the laser duration τ . The photon energy is $\omega = 0.69$ eV. (The results are similar for $\omega = 2.0$ eV.) The empty circles, boxes, and filled circles denote the kinetic energies in the $A_g(1)$, $A_g(2)$, and H_g modes, respectively. Two experimental durations are denoted by two vertical bars (Dexheimer's duration [4] on the left and Bhardwaj's [5] on the right). Inset: Model pendulum. (b) Laser frequency versus pulse duration excitation diagram. The three shaded zones represent the excitation dominated by the $A_g(2)$, $A_g(1)$, and H_g modes. The empty circles, boxes, and filled circles have the same meanings as those in (a). On the right is the energy level scheme of C_{60} .

The above picture finally enables us to explain the difference between those experiments. Two vertical bars in Fig. 2(a) respectively denote the laser durations used in Dexheimer's and Bhardwaj's experiments. Since Dexheimer's duration is shorter than 40 fs, they observed mainly A_g mode excitations; on the other hand, Bhardwaj's, Hohmann's and Boyle's duration are longer than 40 fs, so that they probed mainly H_g , not A_g , modes.

The successful explanation of those contradictory experimental results gives us confidence to systematically build a mode-specific excitation map. Figure 2(b) shows three main excitation regions, each of which is shaded and labeled by a dominant mode: On the left is the $A_g(2)$ mode, in the middle is the $A_g(1)$ mode, and on the right are the H_g modes. On the right side of Fig. 2(b), we show the energy level scheme: h_{1u} is the highest occupied molecular orbital (HOMO), t_{1u} is the lowest unoccupied molecular orbital (LUMO) (dipole forbidden), and t_{1g} is the LUMO+1 (first dipole allowed). We start from the bottom of Fig. 2(b), where the laser energy is away from any major resonance. We notice that from $\omega = 0.5$ to 1.6 eV, the excitation pattern stays the same: on the shortest duration side, the $A_g(2)$ mode dominates, while in the middle, the $A_g(1)$ mode dominates, followed by the H_g mode excitation. These wide regions provide a comfortable zone to target specific modes. What is surprising is that within this region, the period Ω_ν^o (fs) of the most dominant mode ν and its corresponding optimal laser duration τ_ν^o (with which mode ν acquires the maximal possible energy) obey the empirical relation: $\Omega_\nu^o/\tau_\nu^o \approx 3.4$. We find that provided the frequency is off resonant and the laser intensity is weak, this relation is valid. Interestingly, similar effects have been observed before [21]. Pollard *et al.* showed that the optimal pulse duration is 3/10 of the vibrational period, or $\Omega_\nu^o/\tau_\nu^o = 3.3$ [22]. Very recently, Niikura *et al.* again found if the delay between two laser pulses is 1/4 of the vibrational period, the vibrational wave packet will accelerate [23].

There is an important physical reason behind this relation, which can be explained by a model pendulum [see the inset in Fig. 2(a)]. Assume this pendulum has a period of T and initially is in its equilibrium position [24]. The key is that an external field can accelerate it most effectively in the first quarter of its period, i.e., $T/4$ [see the arrow in Fig. 2(a)]; if the field duration is shorter or longer than $T/4$, this pendulum will not achieve the optimal energy. Consequently, the theoretical ratio of the pendulum period to the field duration is four. In practice, the laser does not directly couple to the lattice, but instead it excites the electron which is coupled to the lattice. Consequently, the ratio Ω_ν^o/τ_ν^o slightly deviates from four, as is clear from the relation $\Omega_\nu^o/\tau_\nu^o \approx 3.4$.

As we increase the photon energy close to the first forbidden transition ($h_{1u} \rightarrow t_{1u}$), we see that the $A_g(2)$'s excitation zone spreads over to a longer duration, as it also

does for $A_g(1)$, but the H_g mode region retracts on the short duration front. We know that without the lattice, the above transition is rigorously forbidden, but with the lattice, this virtual transition occurs through the electron-lattice interaction. This is why the laser can directly probe the electron-lattice interaction. If we further increase the laser frequency to the first-dipole-allowed transition ($h_{1u} \rightarrow t_{1g}$), there is a dramatic change in those mode excitations. The vibrational excitation becomes sporadic [see Fig. 2(b)], where the circles and boxes have the same meanings as those in Fig. 2(a). The excitation does not form big islands. Such sporadic mode excitation results from multiple electronic excitations among three closely related states (h_{1u} , t_{1u} , and t_{1g}) and other high-lying states. The major challenge for the resonant excitation is that one does not have a wide range to work with, and the above empirical relation is not applicable. However, the advantage is that it does provide a means to selectively target those otherwise inaccessible normal modes at different laser durations. Therefore, this diagram provides a comprehensive pathway to selectively excite a few phonon modes, which may have important applications in the future. In particular, the current investigations of the K_3C_{60} and Rb_3C_{60} superconductors have been done at a duration of 10 fs, and thus only could access the A_g modes [25]. We suggest that a new experiment with a longer pulse duration should enable one to detect those important H_g modes. More importantly, by changing the temperature through the superconducting transition temperature, individual contributions of these modes to Cooper pairs could be probed and controlled by tuning the laser pulse duration, which is of great importance to ongoing investigations in high- T_c superconductors [2,3]. Experimentally, changing the laser pulse duration is achievable [26].

In conclusion, a previous experimental discrepancy has motivated us to do a numerical simulation to investigate whether one can selectively target a few specific phonon modes. We find that vibrational excitations sensitively depend on the laser pulse duration. Each mode in C_{60} has an optimal duration. For a duration shorter than 40 fs, the A_g modes dominate, but for a duration longer than 40 fs, the H_g modes take over. An excitation diagram is constructed to probe a few specific modes. This may pave the way to control those phonon mode excitations.

The authors would like to thank Professor T. Kobayashi for fruitful discussions and helpful references. They also would like to thank Professor P.B. Corkum for useful discussions. The authors greatly appreciate Professor I.V. Hertel sending them his preprint and unpublished experimental results. This work was supported by the U.S. Army Research Development and Engineering Command Acquisition Center.

- [1] D.S. Chemla and J. Shah, *Nature (London)* **411**, 549 (2001).
- [2] R. A. Kaindl *et al.*, *Science* **287**, 470 (2000); Y. Xu *et al.*, *Phys. Rev. Lett.* **91**, 197004 (2003); J. Demsar *et al.*, *ibid.* **82**, 4918 (1999); S.D. Brorson *et al.*, *ibid.* **64**, 2172 (1990).
- [3] W. Albrecht *et al.*, *Phys. Rev. Lett.* **69**, 1451 (1992); Y. Liu *et al.*, *Appl. Phys. Lett.* **67**, 3022 (1995); O.V. Misochko *et al.*, *Phys. Rev. Lett.* **89**, 067002 (2002); O.V. Misochko, *Phys. Solid State* **42**, 1204 (2000); O.V. Misochko and M.V. Lebedev, *ibid.* **43**, 1195 (2001).
- [4] S. Dexheimer, *et al.*, in *Ultrafast Phenomena VIII*, edited by J.L. Martin, A. Migus, G.A. Mourou, and A.H. Zewail, Springer Ser. Chem. Phys. Vol. 55, (Springer-Verlag, Berlin, 1993) p. 81.
- [5] V.R. Bhardwaj *et al.*, *Phys. Rev. Lett.* **91**, 203004 (2003).
- [6] H. Hohmann *et al.*, *Phys. Rev. Lett.* **73**, 1919 (1994).
- [7] M. Boyle *et al.* (unpublished).
- [8] W.M. You *et al.*, *Phys. Rev. B* **47**, 4765 (1993).
- [9] G. P. Zhang *et al.*, *Phys. Rev. Lett.* **88**, 077401 (2002).
- [10] We are able to accurately reproduce their electron spectrum and vibrational modes frequencies.
- [11] G. P. Zhang and W. Hübner, *Phys. Rev. Lett.* **85**, 3025 (2000).
- [12] G. P. Zhang, *Phys. Rev. Lett.* **91**, 176801 (2003).
- [13] G. P. Zhang *et al.*, *Phys. Rev. B* **68**, 165410 (2003).
- [14] G. P. Zhang *et al.*, *J. Chem. Phys.* **106**, 6398 (1997).
- [15] The experiment does not specifically provide the laser intensity [4].
- [16] The period of kinetic energy is half of the period of the vibration.
- [17] B. Torralva *et al.*, *Phys. Rev. B* **64**, 153105 (2001).
- [18] This result is also true even with the laser intensity up to 0.8 eV/Å.
- [19] For instance, Cina and Smith derived an analytic expression for the ground state population change [see J. A. Cina and T. J. Smith, *J. Chem. Phys.* **98**, 9211 (1993); T. J. Smith and J. A. Cina, *J. Chem. Phys.* **104**, 1272 (1996)]. Also, see R. Kosloff, A. D. Hammerich, and D. Tannor, *Phys. Rev. Lett.* **69**, 2172 (1992); A. M. Wiener, *et al.*, *Science* **247**, 1317 (1990); R. Merlin, *Solid State Commun.* **102**, 207 (1997).
- [20] Our simulation is performed up to 400 fs. Then we find the maximal energy for each mode.
- [21] J. Janszky *et al.*, *Chem. Phys. Lett.* **213**, 368 (1993); J. Janszky and T. Kobayashi, *Opt. Commun.* **76**, 30 (1990); D. M. Jonas *et al.*, *J. Phys. Chem.* **99**, 2594 (1995).
- [22] W. T. Pollard *et al.*, *J. Phys. Chem.* **96**, 6147 (1992).
- [23] H. Niikura, D. M. Villeneuve, and P. B. Corkum, *Phys. Rev. Lett.* **92**, 133002 (2004).
- [24] If the sample's temperature is extremely high, then a distribution of initial zero-point velocities is necessary and more realistic, and our relation may become less accurate. Since phases of vibrations are also different, controlling those vibrations is much more challenging.
- [25] S. B. Fleischer *et al.*, *Appl. Phys. Lett.* **62**, 3241 (1993); **71**, 2734 (1997).
- [26] E. E. B. Campbell *et al.*, *Phys. Rev. Lett.* **84**, 2128 (2000).